Joint Single-and Multi-Beam Angle-Domain NOMA for Hybrid MmWave MIMO Systems

Israa Khaled, Charlotte Langlais, Ammar El Falou, Michel Jezequel, Bachar Elhasssan

Joint Single- and Multi-Beam Angle-Domain NOMA for Hybrid MmWave MIMO Systems

Israa Khaled*†, Charlotte Langlais*, Ammar El Falou†‡, Michel Jezequel*, Bachar ElHasssan†
* IMT Atlantique, Mathematical and Electrical Department, CNRS UMR 6285 Lab-STICC, Brest, France
† Lebanese University, Faculty of Engineering, Tripoli, Lebanon
‡ CEMSE, King Abdullah University of Science and Technology (KAUST), Thuwal, Saudi Arabia

***Abstract*—In this paper, we propose a joint single-beam (SB) and multi-beam (MB) non-orthogonal multiple access (NOMA) scheme with limited feedback for the hybrid millimeter-wave (mmWave) massive multiple-input multiple-output (MIMO) systems. This scheme provides combined advantages with respect to the previous works: i) hybrid beamforming to restrain the number of radio-frequency chains, ii) joint SB- and MB-NOMA to benefit from NOMA multi-user diversity, whatever the load of the cell and the users' position are, iii) limited feedback, with the only knowledge of users' angle information. Specifically, we propose two schemes: the former gives a significant sum-rate performance compared to digital beamforming, while the latter reduces the number of active radio-frequency chains, i.e., the energy consumption. Meanwhile, we develop a low-complex two-stage user grouping strategy by exploiting the joint potential of SB- and MB-NOMA schemes according to the users' angle. Numerical results verify the performance of the proposed schemes using the stochastic mmWave channel model NYUSIM from New York University.**

***Index Terms*—mmWave, massive MIMO, NOMA, hybrid beamforming.**

I. Introduction

The cellular systems exploit new and innovative technologies, such as massive multiple-input multiple-output (m-MIMO), non-orthogonal multiple access (NOMA), and millimeter-wave (mmWave), to meet the incredible demands of high data traffic [1], [2]. Indeed, the short mmWave wavelengths facilitate the deployment of large-scale antenna arrays (LSAAs) in a reasonable size. The m-MIMO system enables high beamforming gain and mitigates the severe mmWave path loss. NOMA efficiently improves the connection by multiplexing users in the power domain and making use of successive interference cancellation (SIC).

The fully digital beamforming (DBF) requires as many radio frequency (RF) chains as transmit antennas and is not feasible with m-MIMO due to high hardware complexity and cost [3]. Instead, hybrid mmWave systems, with limited RF chains deployed to drive LSAAs, have been proposed as a complexity- and cost-effective solution for the possible implementations of mmWave m-MIMO schemes [3]. Another critical issue of m-MIMO is the requirement of a considerable amount of channel state information (CSI) increasing the signaling duration and producing a more extended training sequence. By exploiting the main features of mmWave channels, i.e., high directionality and significant blockage, the user's angle-of-departure (AoD), w.r.t. the base station (BS), is considered as a promising limited feedback [4], [5].

Hybrid beamforming (HBF)-based NOMA systems are extensively studied in the literature [6], [7]. Our study focuses on the angle-domain (AD) MIMO-NOMA, where the users are clustered based on their AoD information w.r.t the BS. Most of the existing works on AD MIMO-NOMA using DBF, HBF, or analog beamforming, partition the users into groups based on their angle difference and form a single-beam (SB) toward each group [4]. However, the beam width is very narrow with LSAAs, and thereby the SB-NOMA schemes can only serve concurrently the users having similar AoD. Accordingly, the number of users served simultaneously by the conventional SB-NOMA is limited, which reduces the performance gain of such a scheme in mmWave hybrid systems with LSAAs. To exploit more degrees of freedom (DoF) and accommodate more users using limited RF chains, the authors in [8] propose a joint SB-NOMA and time division multiple access (TDMA) scheme. Specifically, they develop a group clustering algorithm in the time and space domains that reduces the interference between the SB-NOMA and the single-user (SU) groups in each time slot. While the SB-NOMA-TDMA scheme reduces the complexity and the cost by using HBF, TDMA requires high precision in time synchronization among users since mmWave communications usually provide a high symbol rate. Recently, the authors in [9] discuss the general idea of the multi-beam (MB) NOMA scheme in hybrid mmWave systems, while the authors in [10] offer its implementation details. With the beam splitting technique, the BS forms, within the same RF chain, multiple analog beams to point toward multiple NOMA users with arbitrary AoDs. The authors show that MB-NOMA efficiently exploits the multi-user diversity, unlike SB-NOMA, by performing NOMA transmission even when the users have very separate AoDs. In [11], the authors propose a resource allocation design for MB-NOMA scheme based on full CSI.

In this paper, we propose a joint SB and MB AD-NOMA scheme for hybrid mmWave m-MIMO systems, where only the AoD of each user is fed back to the BS. This scheme provides combined advantages w.r.t. the previous cited works: i) HBF to restrain the number of RF chains (N_{RF}), ii) joint SB- and MB-NOMA to benefit from NOMA multi-user diversity, whatever the load of the cell and the users' position in the cell, iii) limited feedback, with the only knowledge of users' AoD. First, we investigate the performance of

the SB-NOMA and the MB-NOMA schemes for a 2-user scenario. Unlike the previous works on AD HBF-NOMA, we leverage the potentiality of SB-NOMA when the users are very close to each other and the ability of MB-NOMA to accommodate more users with separated AoDs. Second, in a multi-user scenario, we propose the joint SB and MB AD-NOMA scheme where we design a low-complex two-stage user grouping (UG) algorithm. Meanwhile, two different joint SB-MB-NOMA schemes are proposed. While the first one only uses MB-NOMA in an overloaded scenario to deal with the important number of users (w.r.t. N_{RF}), the second one exploits MB-NOMA to reduce the number of active RF chains, i.e., the energy consumption as much as possible. In a realistic propagation mmWave environment NYUSIM [12], the first hybrid scheme gives similar sum-rate, compared to the fully digital MIMO-NOMA, when the number of users is lower than the number of RF chains. For an overloaded cell, the performance of the hybrid joint SB-MB-NOMA is progressively flattening out. However, it remains interesting compared to a classical AD HBF-SB-NOMA scheme, which is only able to manage a number of clusters lower than or equal to the number of RF chains.

Symbol Notations: $\mathbf{A}$ is a matrix, $\mathbf{a}$ is a vector, a is a scalar, $(.)^T$ and $(.)^H$ stand for the transpose and the conjugate transpose, respectively. $\mathcal{N}(\mu, \sigma^2)$ denotes a Gaussian random vector with mean μ and variance σ^2.

II. System Model

We consider a downlink NOMA-based mmWave communication in a multi-user hybrid m-MIMO system, where the BS with $N_{BS} \gg 1$ antennas and $N_{RF} \ll N_{BS}$ RF chains serves $K \ll N_{BS}$ single-antenna users. We adopt a hybrid fully-connected architecture at the BS, where a uniform linear array (ULA) is employed.

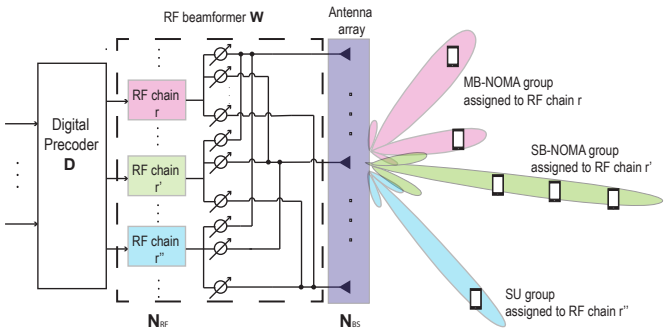

Fig. 1: Joint single- and multi-beam MIMO-NOMA scheme.

A. Channel Model

The multi-path channel vector $\mathbf{h}_k \in \mathbb{C}^{1\times N_{BS}}$ between the BS and the k-th user ($\forall k \in \{1, \cdots, K\} = \mathcal{K}$) can be expressed as

$$h_k = \sum_{l=1}^{L_k} \alpha_{l,k} \mathbf{a}^H(\theta_{l,k}, N_{BS}), \tag{1}$$

where L_k is the number of multi-path components in user k channel, $\alpha_{l,k}$ and $\theta_{l,k}$ are respectively the complex gain and the AoD of the l-th path in user k channel, and $\mathbf{a}(\theta, M) \in \mathbb{C}^{M\times 1}$ is the array steering vector corresponding to the angle θ and the array with M transmit antennas. In this work, we assume that the LoS path exists in the channel of each user. Denote $l = 1$ as the index of the LoS path, i.e., the strongest path. Hence, $\theta_{1,k}$ represents the AoD of user k.

Using ULA with M antennas along the x-axis, the array steering vector $\mathbf{a}(\theta, M)$ corresponding to the angle θ is given by

$$\mathbf{a}(\theta, M) = \left[1, \cdots, e^{j2\pi(M-1)\psi(\theta)}\right]^T = \left[\mathbf{a}^T(\theta, M/2), e^{j2\pi(M/2)\psi(\theta)}\mathbf{a}^T(\theta, M/2)\right]^T, \tag{2}$$

where $\psi(\theta) = \frac{d}{\lambda}\cos(\theta)$, d is the antenna spacing and λ is the wavelength of the transmitted signal.

B. Downlink Transmission Model

The K users are divided into G_{SU} SU groups and G_{SB} multi-user SB-NOMA groups, according to our proposed angle-based multi-user grouping algorithm [5], denoted here as β-SB-NOMA UG. Due to the high beamforming gain driven by LSAAs, few users can be served within the SB-NOMA groups. However, the number of groups that can be simultaneously supported via space division multiple access (SDMA) is limited by the number of RF chains. In order to exploit more DoF especially in an overloaded scenario, i.e., $G_{SU} + G_{SB} > N_{RF}$, we apply the MB-NOMA framework, in which users with arbitrary AoDs can be served within the same group, i.e., by the same RF chain. Specifically, the G_{SU} users are clustered within G'_{SU} SU groups and G_{MB} MB-NOMA groups, such that all the groups can be served simultaneously by the BS without applying additional multiple access technique as TDMA. In other words, the total number $G = G'_{SU} + G_{SB} + G_{MB}$ of groups satisfies that $G \leq N_{RF}$. Denote $\mathcal{S}_g,\ g = 1, \cdots, G$ as the set of users scheduled on the g-th group such that $\bigcup_{g=1}^{G} \mathcal{S}_g = \mathcal{K}$ and $\mathcal{S}_q \bigcap \mathcal{S}_t = \emptyset,\ \forall q \neq t$. We define the user scheduling variable u_k^g as follows

$$u_k^g = \begin{cases} 1 & \text{user k belongs to group g,} \\ 0 & \text{otherwise.} \end{cases} \tag{3}$$

Fig. 1 illustrates the system model of the proposed scheme. Note that each user will be served within one group, i.e., $\sum_{g=1}^{G} u_k^g = 1,\ \forall k \in \mathcal{K}$.

1) Hybrid Beamforming Design: The overall downlink precoding matrix $\mathbf{F}$ is constructed as

$$\mathbf{F} = \mathbf{W}\mathbf{D}, \tag{4}$$

where $\mathbf{D} \in \mathbb{C}^{G\times G}$ is the digital precoding matrix and $\mathbf{W} = [\mathbf{w}_1 \cdots \mathbf{w}_G] \in \mathbb{C}^{N_{BS}\times G}$ is the transmit RF beamforming matrix. In this work, we assume that $\mathbf{D} = \mathbf{I}_G$, then the normalization beamforming factor η is given by $\eta = \frac{1}{\mathrm{Tr}(\mathbf{W}^H\mathbf{W})}$.

The conventional SB-NOMA generates a single beam for each NOMA group. However, for MB-NOMA, the beam splitting technique separates adjacent antennas to form multiple sub-arrays creating an analog beam via each sub-array. In this

work, we assume that each MB-NOMA group serves only two users. In other words, the entire antenna array connected with an RF chain is divided into two sub-arrays with $N_{BS}/2$ antennas to generate two beams; each one is pointed in the AoD of the corresponding user. Therefore, the transmit RF beamformer related to group g depends on its type and is given by

$$\mathbf{w}_g = \begin{cases} \mathbf{a}(\theta_g, N_{BS}) \text{ with } \theta_g = \frac{\min\limits_{k\in\mathcal{S}_g}\{\theta_{1,k}\}+\max\limits_{k\in\mathcal{S}_g}\{\theta_{1,k}\}}{2} & \text{if SB-NOMA [5] with } \mathbf{card}(\mathcal{S}_g)\geq 2, \\ \left[\mathbf{a}^T(\theta_{1,k}, N_{BS}/2), e^{2\pi(N_{BS}/2)\psi(\theta_{1,k'})}\mathbf{a}^T(\theta_{1,k'}, N_{BS}/2)\right]^T & \text{if MB-NOMA with } \mathcal{S}_g=\{k,k'\}, \\ \mathbf{a}(\theta_{1,k}, N_{BS}) & \text{if SU with } \mathcal{S}_g=\{k\}. \end{cases} \tag{5}$$

2) Signal Model: In this paper, we classify the users according to the angle-based user ordering strategy [5] that uses the angle-based channel quality $\breve{\zeta}$, which will be defined later. Without loss of generality, we assume that the users are indexed in the descending order of $\breve{\zeta}$, i.e., $\breve{\zeta}_{k,g} \geq \breve{\zeta}_{k',g'}$ $\forall\ k \leq k'$, $\forall g, g'$.

Assuming a successful SIC decoding, the signal y_k^g received at user k which belongs to group g can be expressed as

$$y_k^g = \sqrt{\eta\gamma_{k,g}p_g}\mathbf{h}_k\mathbf{w}_g s_k + \sum_{k'=1}^{k-1} u_{k'}^g\sqrt{\eta\gamma_{k',g}p_g}\mathbf{h}_k\mathbf{w}_g s_{k'} + \sum_{\substack{g'=1\\g'\neq g}}^{G}\sum_{k'=1}^{K} u_{k'}^{g'}\sqrt{\eta\gamma_{k',g'}p_{g'}}\mathbf{h}_k\mathbf{w}_{g'}s_{k'} + z_k^g, \tag{6}$$

where s_k is the modulated signal relative to user k, p_g is the power allocated to group g, $\gamma_{k,g}$ is the power allocation coefficient assigned to user k belonging to group g such that $\sum_{k=1}^{K} u_k^g\gamma_{k,g} = 1$, and $z_k^g \sim \mathcal{N}(0,\, \sigma_n^2)$ is the additive white Gaussian noise. In this work, we apply the angle-based power allocation proposed in [5] including the inter- and intra-group power allocation.

Accordingly, user k belonging to group g, has the following signal-to-interference-plus-noise ratio (SINR), while decoding his own message

$$\text{SINR}_k^g = \frac{\eta\gamma_{k,g}p_g|\mathbf{h}_k\mathbf{w}_g|^2}{\sum_{k'=1}^{k-1} u_{k'}^g\eta\gamma_{k',g}p_g|\mathbf{h}_k\mathbf{w}_g|^2+\sum_{\substack{g'=1\\g'\neq g}}^{G}\sum_{k'=1}^{K} u_{k'}^{g'}\eta\gamma_{k',g'}p_{g'}|\mathbf{h}_k\mathbf{w}_{g'}|^2+\sigma_n^2}. \tag{7}$$

In (7), the first term in the denominator is the residual intra-group interference after SIC, and the second one is the inter-group interference.

By considering the full CSI-based channel quality metric $\zeta_{k,g}$ defined as the superposed-signal to other-clusters interference plus noise ratio at user k given by

$$\zeta_{k,g} = \frac{\eta p_g|\mathbf{h}_k\mathbf{w}_g|^2}{\sum_{\substack{g'=1\\g'\neq g}}^{G}\sum_{k'=1}^{K} u_{k'}^{g'}\eta\gamma_{k',g'}p_{g'}|\mathbf{h}_k\mathbf{w}_{g'}|^2+\sigma_n^2}, \tag{8}$$

we can rewrite SINR_k^g as follows [5]

$$\text{SINR}_k^g = \frac{\gamma_{k,g}\zeta_{k,g}}{\sum_{\substack{g'=1\\g'\neq g}}^{G}\sum_{k'=1}^{K} u_{k'}^{g'}\gamma_{k',g}\zeta_{k,g}+1} \tag{9}$$

Considering a successful decoding at each user and no propagation error, user k assigned with group g achieves the following data rate R_k^g

$$R_k^g = \log_2(1+\text{SINR}_k^g). \tag{10}$$

In [5], we proposed to simplify the channel quality metric ζ such that only the AoD of each user is used and not the full-CSI. Thus, the angle-based channel quality $\breve{\zeta}$ is extracted from the conventional channel quality ζ by considering the simplifying assumption that the NLOS path gains are negligible compared to those of the LOS path in the mmWave channel. This is reasonable thanks to the high directionality and the potential blockage at mmWave frequencies. Accordingly, $\breve{\zeta}$ is given by [5]

$$\breve{\zeta}_{k,g} = \frac{\eta p_g|\mathbf{a}^H(\theta_{1,k}, N_{BS})\mathbf{w}_g|^2}{\sum_{\substack{g'=1\\g'\neq g}}^{G}\sum_{k'=1}^{K} u_{k'}^{g'}\eta\gamma_{k',g'}p_{g'}|\mathbf{a}^H(\theta_{1,k}, N_{BS})\mathbf{w}_{g'}|^2+\sigma_n^2}, \tag{11}$$

III. 2-USER SCENARIO: SB-NOMA VERSUS MB-NOMA

In this section, we consider only two users served with $N_{BS} = 128$ transmit antennas and $2 \leq N_{RF} \ll N_{BS}$ in a mono-path environment. The AoD θ_1 of the first user is set to $10°$, and we uniformly change the AoD θ_2 of the second user, such that $0° \leq \Delta\theta = \theta_2 - \theta_1 \leq 120°$. In [5], [13], we define an angular-based metric β that gives an insight into the spatial inter-user interference in the mmWave environment and that includes both the angular distance and the main-beam width information. The spatial interference $\beta_{k,k'}$ between user k and user k' is defined as follows [5]

$$\beta_{k,k'} = \frac{1}{N_{BS}}|\mathbf{a}^H(\theta_{1,k}, N_{BS})\mathbf{a}(\theta_{1,k'}, N_{BS})|,\ k,k' \in \mathcal{K}. \tag{12}$$

While SB-NOMA forms a single beam between the two users, MB-NOMA generates two beams, each one is pointed in the AoD of one user by using the beam splitting technique. To investigate the spatial behavior of both schemes in the case of the 2-user scenario, we plot their sum-rate performance versus the angle difference $\Delta\theta$ and the spatial inter-user interference β in Fig. 2.

When the two users are very closed to each other, i.e., $\Delta\theta \to 0$ and $\beta \to 1$, the two beams generated by MB-NOMA are superimposed and forms a single beam, and for that, we find in Fig. 2 that the SB-NOMA and MB-NOMA have the same highest sum-rate performance. When $\Delta\theta < \Omega_1^{3\text{dB}} = 2.25°$[1] and $\beta > 0.217$, SB-NOMA slightly outperforms MB-NOMA. Recall from [5] that for SB-NOMA scheme, $0.217 \leq \beta < 1$ is the useful range where both users are served by the main lobe signal, and thereby the beam misalignment is not severe. Otherwise, when the two users are well separated in the angle domain, the performance of SB-NOMA degrades as $\Delta\theta$ increases due to the severe beam misalignment. For any values of $\Delta\theta > 2.25°$, MB-NOMA

[1]With a ULA of $N_{BS} = 128$ antennas, the 3dB-width $\Omega_1^{3\text{dB}}$ of the beam generated at $\theta_1 = 10°$ is equal to $\Omega_1^{3\text{dB}} = 2.25°$.

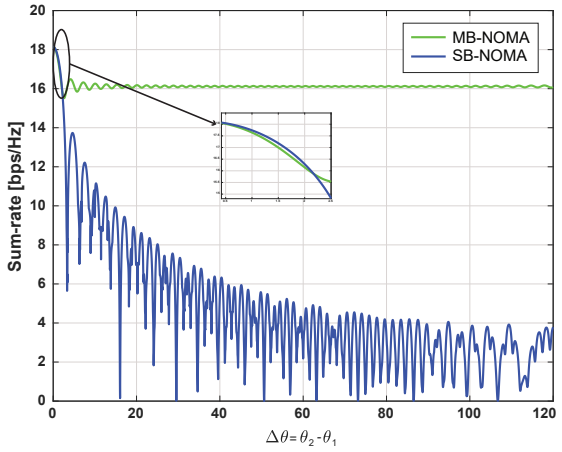

(a) Sum-rate against $\Delta\theta$.

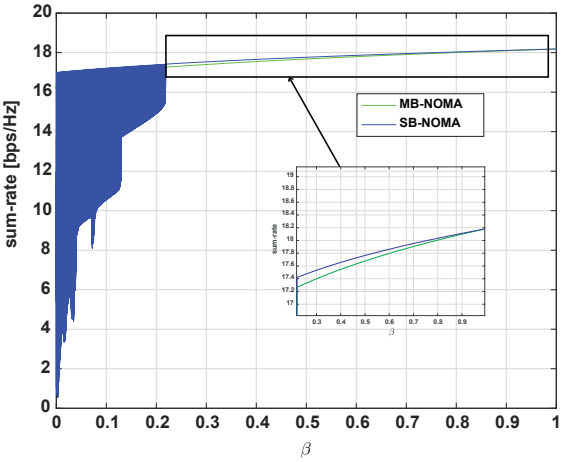

(b) Sum-rate against β.

Fig. 2: SB-NOMA versus MB-NOMA: Sum-rate against $\Delta\theta$ and β.

outperforms SB-NOMA and has approximately a constant sum-rate. Hence, we conclude that SB-NOMA is suitable only when the users are very close to each other. Otherwise, MB-NOMA has a significant constant sum-rate performance independently of $\Delta\theta$, compared to SB-NOMA. Interestingly, from Fig. 2 and by extending to the more general multi-user scenario, it is preferable to cluster first the users with high spatial interference within SB-NOMA groups and then cluster the remaining users in MB-NOMA groups.

IV. Joint SB- and MB-NOMA schemes

In this section, we propose a two-stage UG algorithm for the multi-user hybrid AD MIMO-NOMA systems. In the first stage, we group the users having high spatial interference within the same SB-NOMA group according to β-SB-NOMA UG [5]. It is worth noting that this UG only requires the AoD of users. In the second stage, we partition the remaining users, either 2-by-2 within MB-NOMA or alone in single-user (SU) groups. For the MB-NOMA framework, and according to Section III, users with arbitrary AoDs can be served within the same group, i.e., by the same RF chain. So, finally, in the second stage, MB-NOMA UG partitioned the G_{SU} users into G'_{SU} SU groups and G_{MB} 2-user MB-NOMA groups so that the total number of groups $G = G_{SB} + G'_{SU} + G_{MB}$ satisfies $G \leq N_{RF}$. In this paper, we propose two schemes, namely SB-MB-NOMA and SB-MB-NOMA-RRFC, where the difference only relies upon the second stage.

A. SB-MB-NOMA scheme

In the SB-MB-NOMA scheme, we leverage the SB potential with LSAAs, and we apply MB-NOMA only in an overloaded scenario, i.e., if $G_{SU}+G_{SB} > N_{RF}$ after the first stage. Thus, we partition the G_{SU} users within $G_{MB} = G_{SU} + G_{SB} - N_{RF} > 0$ MB-NOMA groups, and the remaining users are clustered within SU groups. Note that if $G_{SU} + G_{SB} > N_{RF}$ after the first stage, then $G = N_{RF}$ after the second stage.

B. SB-MB-NOMA-RRFC scheme

In the SB-MB-NOMA-**RRFC** scheme, we aim to **R**educe the number of the active **RF C**hains as much as possible. Thereby, we group all the G_{SU} users 2-by-2 in MB-NOMA groups. Hence, $G_{MB} = \lfloor \frac{G_{SU}}{2} \rfloor$ and $G'_{SU} = 0$ (resp. 1) if G_{SU} is even (resp. odd). $\lfloor \cdot \rfloor$ stands for the integer part. The optimal combination of MB-NOMA groups that maximizes the sum-rate can be obtained by exhaustive search over all the possible combinations, whose number is equal to $\prod_{m=1}^{C_{SU}/2}(2*m-1)$ (resp. $\prod_{m=1}^{(C_{SU}+1)/2}(2*m-1)$) if C_{SU} is even (resp. odd).

V. MB-NOMA User Grouping

To reduce the complexity of both schemes, we evaluate three MB-NOMA UG strategies. From Section III, once the users having high spatial interference are clustered into SB-NOMA groups, the choice of associating two users in MB-NOMA according to their AoD is not critical regarding the sum-rate. To this end, we first sort the G_{SU} users in an array in the ascending order of their AoD. Then, we propose three different selection strategies as shown in Fig. 3, denoted as UG1, UG2, and UG3, to select 2-by-2 the users from the sorted array and cluster them in MB-NOMA groups until all the G_{MB} MB-NOMA groups are given. Recall that the value of G_{MB} is calculated according to the scheme type.

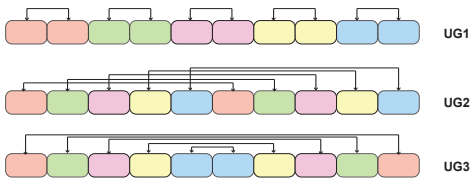

Fig. 3: Three different 2-by-2 selection strategies.

For SB-MB-NOMA-RRFC scheme, the sum-rate performance of the proposed MB-NOMA UG strategies is compared in Fig. 4 with the optimal exhaustive search method, denoted as OPT UG, and the random MB-NOMA UG, where the users are randomly clustered in MB-NOMA groups. Because of memory size limit, we plot the sum-rate of the OPT UG until $K = 10$. Note that the particular form of the curves, especially for a low number of users, is not a result of the number of realizations but related to the number of users being odd or

even. Indeed, for a low number of users, it is more probably that users are well separated in the angle domain and then all are clustered in SU groups after the first stage, i.e., $G_{SU} = K$. Thus, if K is even (resp. odd), there exist $G'_{SU} = 0$ (resp. 1) user served via SDMA. For that, it is obvious that the sum-rate decreases slowly when passing from $K = 2 * Q$ to $K = 2 * Q + 1$ in case of sparse cell, because of the potential of SDMA with LSAAs which enables high beamforming gain. Moreover, it is seen from Fig. 4 that UG1 is closer to OPT UG than the others. This superiority is because of the lower inter-cluster interference achieved when using UG1 compared to UG2 and UG3. In Section VI, UG1 is considered as the reference.

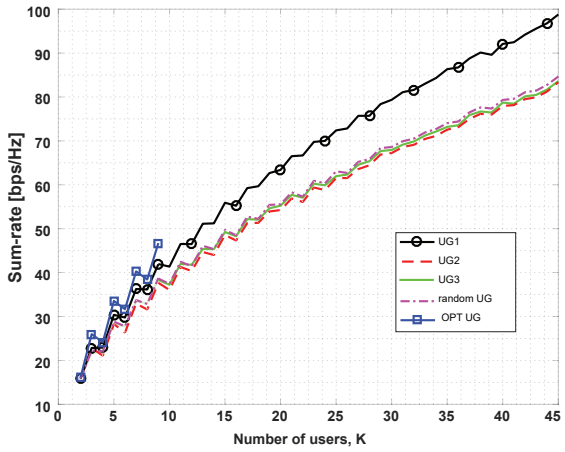

Fig. 4: The sum-rate performance of different MB-NOMA UG algorithms versus the number of users for the SB-MB-NOMA-RRFC scheme. The sum-rate is averaged over 5,000 trials.

VI. Simulation Results

In this section, extensive simulations are performed to verify the performance of the joint SB- and MB-NOMA schemes proposed for hybrid mmWave systems. The performance assessment is done in a multi-path rural environment using the stochastic mmWave channel simulator, called NYUSIM [12], which adopts the time-cluster spatial-lobe approach. Specifically, the simulation parameters are given in Table I.

TABLE I: Simulation parameters

Number of transmit antennas, M	128
Number of RF chains, N_{RF}	16
Carrier frequency	28 GHz
Channel bandwidth, B	20 MHz
Cell edge radius	100 m
Transmission power, P_e	30 dBm
Noise power, σ_n^2	-101 dBm
Minimum SIC power difference, $P_{\min}$	1 mW
Number of paths per time cluster in a rural environment	$\in \{1, 2\}$

To illustrate the advantages of the proposed SB-MB-NOMA and SB-MB-NOMA-RRFC schemes with the angular information, we adopt three baseline schemes; two schemes apply fully DBF (thus requiring $N_{RF} = N_{BS}$) and the other uses HBF: 1) the conventional AD-DBF scheme considered in [14], where the BS generates K directive beams, each one is steered in the AoD of the intended user. 2) DBF-based SB-NOMA scheme proposed in [5], where the β-SB-NOMA UG algorithm clustered the users within SU and SB-NOMA groups 3) HBF-based SB-NOMA-TDMA [8], where the authors propose a simple AD UG strategy, in which UEs with the same estimated angle are clustered within the same group[2]. However, due to the limited RF chains, the authors developed a group clustering algorithm in time-domain that reduces the inter-group interference by clustering the groups with close angular distances in two distinct time slots. In addition, for HBF-SB-NOMA, we apply the same user ordering and power allocation strategies proposed in [5] that uses only the angular information, i.e., users' AoD.

Fig. 5 and Fig. 6 illustrate respectively the average sum-rate and number of active RF chains per time slot versus the number of users for the different aforementioned schemes. We recall that all schemes only need the AoD of each user.

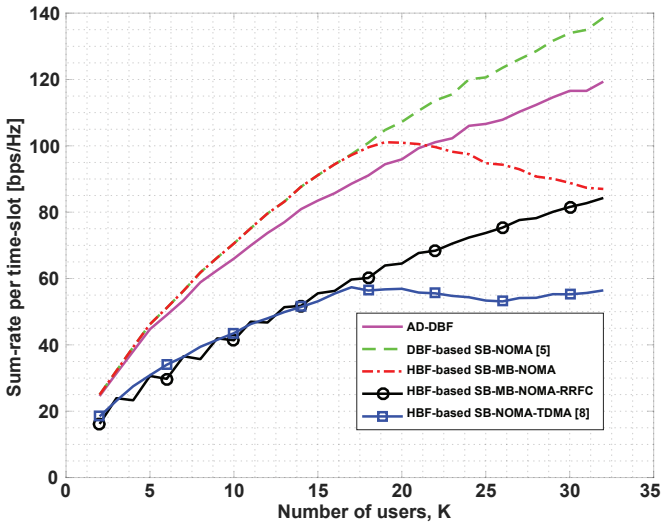

Fig. 5: The sum-rate performance versus the number of users for the different schemes. The sum-rate is averaged over 5,000 trials.

As seen in Fig. 5, the implementation of NOMA, such as DBF-based SB-NOMA, improves the performance of the AD-DBF scheme especially in a congested cell. This is due to the ability of the β-SB-NOMA UG algorithm to cluster users with large spatial interference and the potential of the NOMA technique to reduce this interference. Moreover, with $128/16 = 8$ times less RF chains, HBF-based SB-MB-NOMA outperforms AD-DBF for $K < 24$. Otherwise, AD-DBF outperforms HBF-based SB-MB-NOMA at the expense of high cost and prohibitive complexity. Indeed, as shown in Fig. 6, for HBF-based SB-MB-NOMA, the number of active RF chains, i.e., the number of groups, is equal to $N_{RF} = 16$ while the number of active RF chains for AD-DBF is always equal to the number of antennas $N_{BS} = 128$ whatever the number of groups.

[2]Note that the estimated angles belong to a predefined angle set with a fixed search step size $J = N_{BS}$ [8].

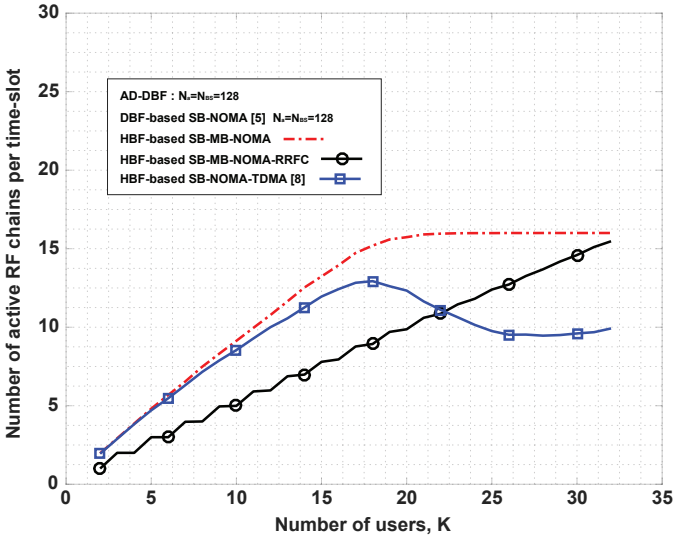

Fig. 6: The number N_a of active RF chains per time slot versus the number of users for the different schemes. This number is averaged over 5,000 trials.

For $K \leq N_{RF}$, it is already known that HBF-NOMA (represented by the performance of HBF-based SB-MB-NOMA) is preferable to DBF-NOMA since the hybrid scheme has the same performance with a lower complexity and a lower cost. However, in a congested cell, the proposed HBF-based SB-MB-NOMA scheme offers new DoFs to compensate for the few RF chains and provides user connectivity even if $K > N_{RF}$.

From Fig. 5, we observe a constant increasing of the sum-rate of HBF-SB-MB-NOMA with the number of users, until $K \leq N_{RF}$, then a decreasing performance. Indeed, HBF-SB-NOMA supports SU and SB-NOMA groups with low spatial interference due to the narrow beam of LSAAs. However, when $K > N_{RF}$, the remaining SU groups obtained after the first stage are regrouped between SU and 2-user MB-NOMA groups. Since the beamforming gain of the multi-beam groups is reduced compared to single-beam, the sum-rate performance of SB-MB-NOMA degrades with the increase of K, i.e., the increasing number of MB-NOMA groups.

Moreover, when $K \leq N_{RF}$, the gap in terms of sum-rate between HBF-SB-MB-NOMA and HBF-SB-MB-NOMA-RRFC increases with the number of users, K. Indeed, it is seen from Fig. 6 that the number of active RF chains increases more slowly int the case of RRFC. When the maximum of RF chains is used by SB-MB-NOMA, its sum-rate performance starts to decrease with the number of users, whereas SB-MB-NOMA-RRFC still has some new RF chains to activate. Finally, when $K = 32$, both schemes become similar because they use the same number of RF chains, and provides the same number of groups including SU, SB- and MB-NOMA groups. We observe that SB- MB-NOMA-RRFC clearly succeeds in reducing the number of active RF chains, i.e., the energy consumption compared to the other schemes.

Finally, we find that both SB-MB-NOMA and SB-MB-NOMA-RRFC schemes outperforms NOMA-TDMA [8] in terms of average sum-rate per time slot. Indeed, the users in [8] are served by beams pointed at angles that belong to a predefined set. Thus, such a system suffers from severe beam misalignment. On the other hand, the MB-NOMA schemes leverage the additional degrees of freedom brought by the power domain for multiple access, while TDMA divides the time resource block to serve all the groups.

VII. Conclusion

In this paper, a new joint SB- and MB-NOMA is proposed for hybrid mmWave communication, using only the angular information. This scheme benefits from NOMA multi-user diversity, whatever are the load of the cell and the users' position. Specifically, we propose a low-complex two-stage user grouping algorithm that reduces the inter-user interference in the first stage and aims to add more degrees of freedom in the second stage by exploiting the MB-NOMA framework in mmWave environment. As future work, it would be interesting to design a resource allocation technique including angle, antenna and power allocation techniques for the joint SB- and MB-NOMA scheme in hybrid mmWave m-MIMO systems.

References

[1] R. W. Heath, N. Gonzalez-Prelcic, S. Rangan, W. Roh, and A. M. Sayeed, "An overview of signal processing techniques for millimeter wave MIMO systems," *IEEE J. Sel. Topics Signal Process.*, vol. 10, no. 3, pp. 436–453, 2016.

[2] L. Dai, B. Wang, Y. Yuan, S. Han, I. Chih-Lin, and Z. Wang, "Non-orthogonal multiple access for 5G: solutions, challenges, opportunities, and future research trends," *IEEE Commun. Mag.*, vol. 53, no. 9, pp. 74–81, 2015.

[3] A. F. Molisch, V. V. Ratnam, S. Han, Z. Li, S. L. H. Nguyen, L. Li, and K. Haneda, "Hybrid beamforming for massive MIMO: A survey," *IEEE Commun. Mag.*, vol. 55, no. 9, pp. 134–141, 2017.

[4] Z. Ding, P. Fan, and H. V. Poor, "Random beamforming in millimeter-wave NOMA networks," *IEEE access*, vol. 5, pp. 7667–7681, 2017.

[5] I. Khaled, C. Langlais, A. El Falou, B. ElHassan, and M. Jezequel, "Multi-user angle-domain MIMO-NOMA system for mmwave communications," *IEEE Access*, 2021.

[6] L. Pang, W. Wu, Y. Zhang, Y. Yuan, Y. Chen, A. Wang, and J. Li, "Joint power allocation and hybrid beamforming for downlink mmwave-NOMA systems," *IEEE Trans. Veh. Technol.*, 2021.

[7] A. A. Badrudeen, C. Y. Leow, and S. Won, "Sub-connected structure hybrid precoding for millimeter-wave NOMA communications," *IEEE Wireless Commun. Lett.*, vol. 10, no. 6, pp. 1334–1338, 2021.

[8] X. Hu, C. Zhong, Y. Han, X. Chen, J. Zhao, and Z. Zhang, "Angle-domain mmwave MIMO NOMA systems: analysis and design," in *Proc. IEEE Int. Conf. Commun. (ICC)*, 2019.

[9] L. Zhu, Z. Xiao, X.-G. Xia, and D. O. Wu, "Millimeter-wave communications with non-orthogonal multiple access for B5G/6G," *IEEE Access*, vol. 7, pp. 116 123–116 132, 2019.

[10] Z. Wei, L. Zhao, J. Guo, D. W. K. Ng, and J. Yuan, "A multi-beam noma framework for hybrid mmwave systems," in *Proc. IEEE Int. Conf. Commun. (ICC)*. IEEE, 2018.

[11] ——, "Multi-beam NOMA for hybrid mmwave systems," *IEEE Trans. Commun.*, vol. 67, no. 2, pp. 1705–1719, 2018.

[12] M. K. Samimi and T. S. Rappaport, "3-D millimeter-wave statistical channel model for 5G wireless system design," *IEEE Trans. Microw. Theory Tech.*, vol. 64, no. 7, pp. 2207–2225, 2016.

[13] I. Khaled, C. Langlais, A. El Falou, M. Jezequel, and B. ElHasssan, "Joint SDMA and power-domain NOMA system for multi-user mm-Wave communications," in *Proc. IEEE Int. Wireless Commun. and Mobile Computing (IWCMC)*, 2020, pp. 1112–1117.

[14] I. Khaled, A. El Falou, C. Langlais, B. ElHassan, and M. Jezequel, "Multi-user digital beamforming based on path angle information for mm-Wave MIMO systems," in *Proc. Int. ITG Workshop on Smart Antennas (WSA)*. VDE, 2020.